over an area of about 7×10^3 cm^2. If we extrapolate conservatively over the eastern gulf (an area of about 8×10^5 cm^2), we estimate that about 650,000 metric tons of the black magnetic particles would be raining out per year. This figure is orders of magnitude higher than estimates of rates of infall of iron meteoritic material over the entire earth (*2*). Although the flux is probably spotty, not constant, and limited to an area considerably less than the whole of the eastern gulf, it is significant.

The above lines of evidence indicate that the source of most of these spherules is probably industrial. Parkin *et al.* (*10*) detected a small proportion of black (magnetite) fly ash spherules (0.2 part per thousand) in their airborne dust collections; these spherules were thought to be derived from coal-burning facilities. Handy and Davidson (*12*) have remarked upon the similarity between meteoritic dust and fly ash. Therefore, the black magnetic spherules raining into the eastern gulf and western Florida are probably derived from coal-burning power plants bordering the eastern gulf and from the heavy concentration of industrial facilities which utilize coal and coke in the areas bordering the northern and northeastern gulf. Parkin *et al.* (*10*) have estimated the sedimentation rate in the North Atlantic Ocean from fly ash pollution at only 1 mg/cm^2 per 10^3 years, or 0.01 mm per 10^3 years. On the basis of our calculations, the contribution of black iron magnetic particles alone could be greater than that found by Parkin *et al.* for all fly ash pollutants to the North Atlantic Ocean (magnetite spherules make up only a small percentage of the total solids pollution in the atmosphere). The presence of black metallic spherules in such quantities in the eastern gulf may signify a much more serious particulate pollution, especially on the West Florida continental margin which is relatively isolated from any input of clastic sediment. If the flux of airborne magnetic metallic particles were even two orders of magnitude less than our extrapolation to the eastern gulf, it would contribute about as much particulate Fe per year as the 14 rivers with significant flow that empty into the gulf on the western Florida coast; this estimate is based upon the mean annual discharges and mean Fe contents of these rivers (*13*).

The internal structures of interlocking plates that we observed in the noncosmic particles (probably fly ash) from the eastern gulf (see Fig. 1, B and C) are similar to those described by Aumento and Mitchell (*6*) as characteristic of cosmically derived particles. It follows that any predominantly molten iron droplet thrown into the atmosphere from a terrestrial or nonterrestrial source may develop similar internal structures, which therefore are not diagnostic of origin. Great care must be taken in studies of cosmic particles to assure that samples from the air, in the water column, or in the sediments are not contaminated by industrially derived particles. Even large particles (up to 800 μm) deep within the sediment may be suspect; particles may migrate slowly down into the sediments as a result of animal reworking, thus contaminating the upper portions of cores.

We have found some large particles (up to 800 μm in diameter) hundreds of kilometers from potential industrial source areas. Handy and Davidson (*12*) pointed out that most smokestacks are designed to transport the fly ash high into the air. They reported smog, containing particles up to 200 μm in diameter, at altitudes of over 6000 m in the Chicago area, and they pointed out that convection currents have been known to carry terrestrial dust as high as 11,000 m. Even large metallic spherules of high density would require many hours to fall from such heights, and in that time particles could be transported several hundred kilometers by winds from the point at which they were introduced.

Industrially derived black magnetic spherules pose a problem for studies of particulate Fe concentrations in water masses, in recent sediments, in the atmosphere, and even on the surfaces of older rocks. In many studies it may be necessary to determine the chemical composition of virtually each "cosmic" particle in order to establish that its source is extraterrestrial. One wonders how many studies of micrometeorites and cosmic particles have really dealt with a component of fly ash.

LARRY J. DOYLE
THOMAS L. HOPKINS
PETER R. BETZER

Department of Marine Science, University of South Florida, St. Petersburg 33701

References and Notes

1. D. W. Eggiman and P. R. Betzer, *Anal. Chem.* **48**, 886 (1976).
2. R. A. Schmidt, *A Survey of Data on Microscopic Extraterrestrial Particles* (National Aeronautics and Space Administration, Washington, D.C., 1965).
3. H. Pettersson and K. Fredriksson, *Pac. Sci.* **12**, 71 (1958); W. Hunter and D. W. Parkin, *Proc. Roy. Soc. London* **255**, 382 (1960); W. D. Crozier, *J. Geophys. Res.* **65**, 2971 (1960).
4. J. Murray and A. G. Renard, *Proc. R. Soc. Edinburgh* **12**, 474 (1884).
5. R. B. Finkelman, *Science* **167**, 982 (1970).
6. F. Aumento and W. S. Mitchell, *Geology* **3**, 407 (1975).
7. V. B. Marvin and M. T. Einaudi, *Geochim. Cosmochim. Acta* **31**, 1871 (1967).
8. P. W. Hodge, F. W. Wright, C. C. Langway, Jr., *J. Geophys. Res.* **69**, 2919 (1964); A. El Gorsey, *Contrib. Mineral. Petrol.* **17**, 331 (1968).
9. O. Vittori, *Pure Appl. Geophys.* **69**, 360 (1968); M. Del Monte, T. Wanni, M. Tagliazucca, *J. Geophys. Res.* **79**, 4375 (1974).
10. D. W. Parkin, D. R. Phillips, R. A. L. Sullivan, *J. Geophys. Res.* **75**, 1782 (1970).
11. H. T. Millard, Jr., and R. B. Finkelman, *ibid.* **75**, 2125 (1970).
12. R. L. Handy and D. T. Davidson, *Proc. Iowa Acad. Sci.* **60**, 373 (1953).
13. D. F. Martin, M. T. Doig III, R. H. Pierce, Jr., "Distribution of naturally occurring chelators (humic acids) and selected trace metals in some west coast Florida streams, 1968–1969" (Professional Papers Series 12, Florida Department of Natural Resources, Marine Research Laboratory, St. Petersburg, April 1971).
14. We thank T. Pyle, K. Sprecher, and D. Milliken who aided in sample collection. Chemical analyses were supported by Office of Naval Research grant N00014-75-C-0539. W. C. Meyer took the SEM photos.

6 May 1976; revised 25 August 1976

Electron Plasma Oscillations Associated with Type III Radio Bursts

Abstract. *Plasma wave electric field measurements with the solar orbiting Helios spacecraft have shown that intense (approximately 10 millivolts per meter) electron plasma oscillations occur in association with type III solar radio bursts. These observations confirm the basic mechanism, proposed in 1958, that type III radio emissions are produced by intense electron plasma oscillations excited in the solor corona by electrons ejected from a solar flare.*

Plasma wave electric field instruments on the German-American Helios 1 and Helios 2 spacecraft, in orbit around the sun, have detected intense electron plasma oscillations in association with type III solar radio bursts. These observations confirm a well-known mechanism, proposed by Ginzburg and Zheleznyakov (*1*) in 1958, for the generation of these radio emissions. In this report we briefly describe the essential features of the plasma oscillation mechanism for generating type III radio bursts and present the recent Helios results, which show the occurrence of intense electron plasma oscillations in association with type III radio bursts.

Type III radio bursts are produced by particles ejected from a solar flare and are characterized by an emission frequency which decreases with increasing time. These radio bursts are observed over a very broad frequency range, from as high as several hundred megahertz to as low as 10 khz. The characteristic frequency variation of type III radio bursts was explained by Wild (2) in 1950, who proposed that the radio emissions are generated at a local oscillation frequency of plasma in the solar corona called the electron plasma frequency: $f_p^- = 9n^{\frac{1}{2}}$ (khz), where n is the electron density (cm^{-3}). The decreasing emission frequency with increasing time is attributed to the decreasing electron density, hence plasma frequency, encountered by the solar flare particles as they move outward through the solar corona and solar wind. Measurements with satellite-borne instruments have shown that the particles responsible for the type III radio emissions are electrons with energies ranging from a few kiloelectron volts to several tens of kiloelectron volts (3).

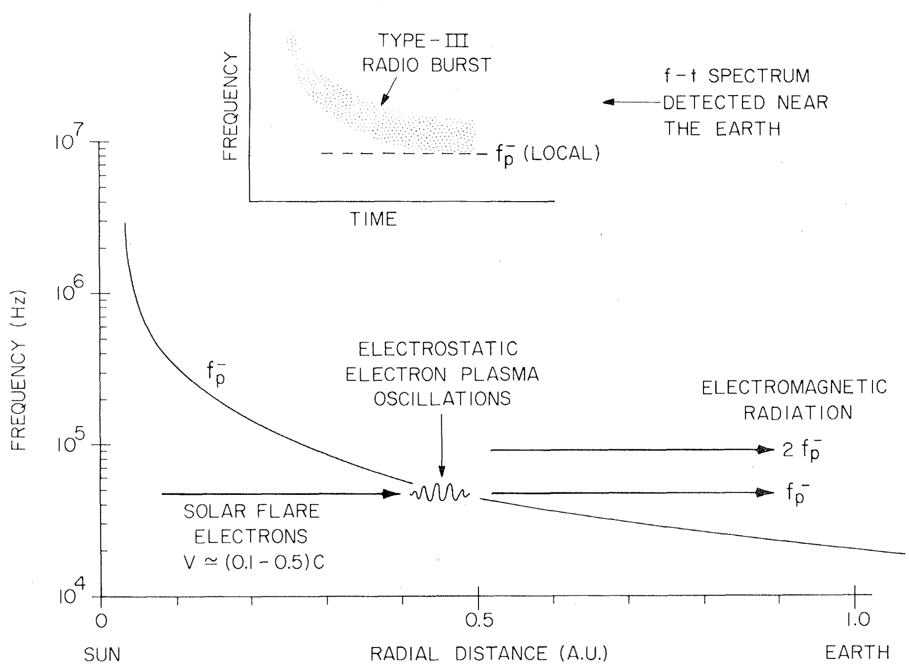

Fig. 1. Radial variation of the electron plasma frequency, f_p^-, between the sun and the earth. Type III solar radio bursts are believed to be generated by a two-step process in which (i) localized electron plasma oscillations at f_p^- are produced by solar flare electrons streaming outward from the sun, and (ii) these plasma oscillations are converted to escaping electromagnetic radiation by nonlinear wave-wave interactions. The characteristic frequency variation of the type III burst is caused by the decreasing plasma frequency encountered by the solar flare electrons as they move away from the sun. Abbreviations: v, electron velocity; c, speed of light.

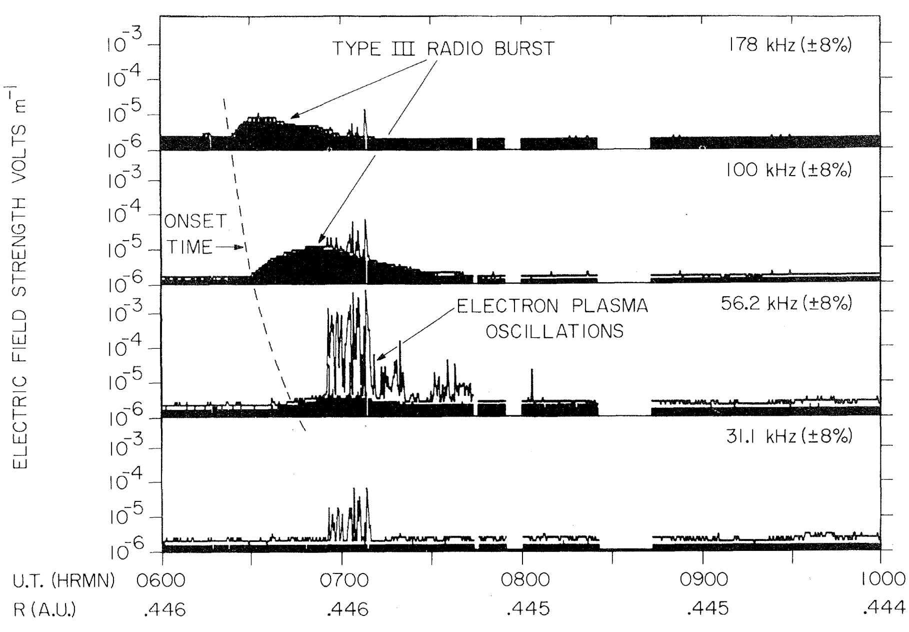

Fig. 2. Example of the intense electron plasma detected by Helios 2 in association with a type III solar radio burst. Note the characteristic increasing onset time of the type III burst with decreasing frequency and the narrow bandwidth of the electron plasma oscillations in the 56.2-khz channel. The electron plasma frequency determined by the solar-wind plasma experiment on Helios is $f_p^- = 54$ khz, which is very close to the observed frequency of the electron plasma oscillations. The solid lines give the peak electric field intensities, and the solid black area indicates the average intensities.

According to the mechanism proposed by Ginzburg and Zheleznyakov, and subsequently refined and modified by other investigators (4, 5), the generation of type III radio emissions is a two-step process in which (i) electrostatic plasma oscillations are first produced at the local electron plasma frequency by a two-stream instability excited by the solar flare electrons, and (ii) the plasma oscillations are converted to electromagnetic radiation by nonlinear wave-wave interactions. This mechanism is illustrated schematically in Fig. 1, which shows a model for the radial variation of the electron plasma frequency from the sun to the earth. According to current ideas, the electrostatic energy of the plasma oscillations is transformed into electromagnetic radiation at either the fundamental (f_p^-) or the harmonic ($2f_p^-$) of the local electron plasma frequency. The radiation at the fundamental is caused by interactions of the plasma oscillations with ion sound waves, and the radiation at the second harmonic is caused by interactions between oppositely propagating electron plasma oscillations. Radiation at both the fundamental and the harmonic has been detected, although at low frequencies ($\lesssim$ 1 Mhz) the harmonic radiation appears to be the dominant component (6).

Since the electron plasma oscillations are local phenomena and cannot be detected remotely, in situ measurements must be obtained in the solar corona or solar wind to confirm the occurrence of these oscillations in association with type III bursts. Rough estimates, using the theoretical model of Papadopoulos *et al.* (5), indicate that plasma oscillations with field strengths of about 10 mv m^{-1} or larger are required to explain the power flux of a typical type III radio burst at low frequencies (7). Although it should be possible to detect such plasma oscillations in the solar wind with earth-orbiting satellites, considerable difficulty has been experienced in obtaining confirming observations. After nearly 4 years of measurements with the earth-orbiting IMP 6 and IMP 8 satellites, no electron plasma oscillations with intensities this large have been found in association with a type III radio burst (7). This difficulty can be attributed to two factors. First, since the plasma oscillations occur only in the source, whereas the type III radiation propagates over large distances, electron plasma oscillations are expected to be detected for only a small fraction of the observable type III radio bursts. If the source region is very small or filamentary, as appears to be the case, then it is very improbable that the spacecraft will be suitably located within the beam of electrons ejected by the flare to detect the plasma oscillations. Second, and probably more important, for satellite observations near the earth it is very difficult to distinguish plasma oscillations generated by electrons from a solar flare from similar plasma oscillations (8) generated in the vicinity of the earth by electrons emitted from the earth's bow shock. The noisy and very disturbed plasma environment near the earth makes it very difficult to identify the plasma oscillations expected in association with a type III radio burst.

The solar orbiting Helios 1 and Helios 2 spacecraft provided the first opportunity to obtain simultaneous measurements of plasma waves and radio emissions away from the disturbing effects of the earth and in the region close to the sun, where the solar radio bursts are most intense. These spacecraft were launched on 10 December 1974 and 15 January 1976 into eccentric orbits near the ecliptic plane with perihelion radial distances of 0.309 and 0.290 A.U., approaching closer to the sun than any previous spacecraft. The plasma wave and radio astronomy instrumentation on the Helios spacecraft consists of a 32-m electric dipole antenna and a combination of frequency spectrum analyzers provided by the University of Iowa, the University of Minnesota, and Goddard Space Flight Center. A more detailed description of this instrumentation is provided by Gurnett and Anderson (9).

During the first 18 months after the launch of Helios 1, a total of 24 type III radio bursts was detected by the two Helios spacecraft. Of these, three events have been found with unusually intense electron plasma oscillations, which are almost certainly associated with the type III radio emission. The basic parameters for these events are summarized in Table 1. All three of these events were detected by Helios 2 within a single 24-hour interval from 31 March to 1 April 1976, during a period of exceptional solar flare activity which lasted from 23 March to 2 April 1976. At the time of these events Helios 2 was at a radial distance of about 0.45 A.U. from the sun and in a position which placed the spacecraft within, or very near, the source region of the type III radio emission.

Table 1. Type III radio bursts associated with intense electron plasma oscillations detected by Helios 1 and Helios 2 spacecraft. The values in the last column are the plasma oscillation field strengths required to account for the observed radio emission intensities; they were computed by using the theory of Papadopoulos *et al.* (5) with $\alpha = 0.1$, $n = 36$ electron/cm^3, $T_e = 10$ ev, and $R = 0.44$ A.U. [see (7) for details of these calculations].

Type III burst: Date (1976)	Type III burst: U.T.	Type III burst: Intensity at $2f_p^- \simeq 100$ khz (watt m^{-2} hertz^{-1})	f_p^- (khz)	Electric field strength of plasma oscillations (mv m^{-1}): Observed	Electric field strength of plasma oscillations (mv m^{-1}): Calculated
31 March	1810	1.15×10^{-17}	58	14.8	6.01
1 April	0620	2.59×10^{-17}	54	5.26	7.37
1 April	1038	8.17×10^{-17}	56	2.35	9.82

The detailed electric field intensities for one of these events are shown in Fig. 2. The type III radio emission can be clearly seen in the 178- and 100-khz channels and is just barely detectable in the 56.2-khz channel. The smooth intensity variation and the increase of onset time with decreasing frequency provide a unique identification of this event as a type III radio burst. Starting at about 0655 U.T., and lasting to about 0720 U.T., a series of intense bursts of electric field noise is evident in the 56.2-khz channel. These bursts are very intense, reaching a peak electric field strength of 5.26 mv m^{-1}. This intensity is almost 60 db greater than the corresponding intensity of the type III radio emission in this channel. Comparisons with the solar wind plasma density measurements from Helios (10) show that the center frequency of these bursts, ~ 56.2 khz, is very close to the local electron plasma frequency, $f_p^- = 54$ khz. The bandwidth of these bursts is evidently very narrow, since the corresponding weak bursts in the adjacent 31.1- and 100-khz channels can be completely attributed to the frequency response of the spectrum analyzer filters, assuming a nearly monochromatic emission at $f_p^- \simeq 54$ khz. The narrow bandwidth of the bursts and the close agreement of the emission frequency with the local electron plasma frequency provide convincing evidence that this electric field noise consists of electron plasma oscillations. The very close temporal correspondence between the occurrence of these plasma oscillations and the occurrence of the type III radio burst leaves essentially no doubt that the plasma oscillations are associated with the type III emission. A qualitatively similar relationship is also observed for the remaining two events.

The peak electric field strengths of the three intense plasma oscillation events detected by Helios and the corresponding type III radio emission intensities at $2f_p^- \simeq 100$ khz are summarized in Table 1. For comparison, the computed plasma oscillation field strengths required to account for the observed radio emission intensities are also shown in Table 1. These electric field intensities have been calculated by using the theoretical model of Papadopoulos *et al.* (5) for the conversion of the plasma oscillation energy to electromagnetic radiation. Further details of the assumptions used in these calculations are given by Gurnett and Frank (7). As can be seen from Table 1, the observed plasma oscillation field strengths are in excellent quantitative agreement with the field strengths required by the theory.

The Helios observations have provided a firm confirmation that the basic plasma oscillation mechanism proposed by Ginzburg and Zheleznyakov is involved in the generation of type III radio emissions. However, many important questions still remain. Since intense plasma oscillations of the type detected by Helios are rarely observed compared to the number of type III radio bursts detected at the earth (7), it is generally concluded that the spatial distribution of plasma oscillations must be highly inhomogeneous, with the intense plasma oscillations confined to small isolated regions. Since the power radiated by the plasma oscillations is a very strong function (fourth power) of the electric field strength, the fraction of the total volume containing plasma oscillations could be quite small, < 1 percent, with only a moderate increase in the required field strengths. For each of the three cases detected by Helios the plasma oscillations are extremely impulsive, consisting of many short bursts lasting for only a few seconds or less. These impulsive variations are clearly indicated by the large ratio of the peak to average field strengths evident in Fig. 2. The highly inhomogeneous structure indicated by these variations was not contemplated in the original model of Ginzburg and Zheleznyakov, which only dealt with the linear growth of the plasma oscillations, and has been studied only recently (*5*) in relation to the large-amplitude nonlinear evolution of the two-stream instability. Considerable further investigation, both theoretical and experimental, is still required to fully understand the spatial structure of these intense plasma oscillations and the implications with regard to the generation of radio emissions by the sun and other cosmic radio sources.

DONALD A. GURNETT
ROGER R. ANDERSON
Department of Physics and Astronomy, University of Iowa, Iowa City 52242

References and Notes

1. V. L. Ginzburg and V. V. Zheleznyakov, *Sov. Astron. AJ* **2**, 653 (1958).
2. J. P. Wild, *Aust. J. Sci. Res. Ser. A* **3**, 541 (1950).
3. L. A. Frank and D. A. Gurnett, *Sol. Phys.* **27**, 446 (1972); H. Alvarez, F. Haddock, R. P. Lin, *ibid.* **26**, 468 (1972); R. P. Lin, L. G. Evans, J. Fainberg, *Astrophys. Lett.* **14**, 191 (1973).
4. P. A. Sturrock, *Nature (London)* **192**, 58 (1961); D. A. Tidman, T. J. Birmingham, H. M. Stainer, *Astrophys. J.* **146**, 207 (1966); S. A. Kaplan and V. N. Tsytovich, *Sov. Astron. AJ* **11**, 956 (1968); D. F. Smith, *Space Sci. Rev.* **16**, 91 (1974).
5. K. Papadopoulos, M. L. Goldstein, R. A. Smith, *Astrophys. J.* **190**, 175 (1974).
6. M. L. Kaiser, *Sol. Phys.* **35**, 181 (1975).
7. D. A. Gurnett and L. A. Frank, *ibid.*, p. 477.
8. F. L. Scarf, R. W. Fredricks, L. A. Frank, M. Neugebauer, *J. Geophys. Res.* **76**, 5162 (1971).
9. D. A. Gurnett and R. R. Anderson, *ibid.*, in press.
10. We thank H. Rosenbauer and R. Schwenn from the Max-Planck-Institut for providing the plasma density data from Helios.
11. Research at the University of Iowa was supported by NASA contract NAS5-11279 and grant NGL-16-001-043. Research was performed by D.A.G. while on leave at the Max-Planck-Institut für Extraterrestrische Physik, Garching bei München, West Germany. Research at the Max-Planck-Institut was supported by the Alexander von Humboldt Foundation.

14 July 1976; revised 8 October 1976

Elemental Analysis of Biological Specimens in Air with a Proton Microprobe

Abstract. *The unique capabilities of the proton microprobe in an atmospheric environment as a biological tool are illustrated in studies of arsenic and mercury distributions in single strands of hair from poisoning victims and of the distributions of several abundant elements in frozen hydrated eye and kidney specimens from rats.*

In an earlier report (*1*) we described the capabilities of the scanning proton microprobe to map out the spatial distributions of a given element (or elements), even at trace concentrations, using a 2-Mev collimated proton microbeam emergent into air. With this technique, the sample is mechanically scanned in front of the stationary microbeam while an energy-dispersive x-ray detector collects proton-induced x-rays characteristic of the elemental species being excited by the microbeam at each instant. This information can be displayed on a conventional oscilloscope if the trace is moved in synchronization with the sample motion, brightening the spot when x-rays of a particular energy are detected; alternatively, the information can be stored in a multichannel scaler or computer memory for subsequent analysis. The latter procedure is particularly convenient when a one-dimensional scan is made repeatedly across a sample, since one obtains a graph of the abundance of each element versus position along the scan direction. We have found this method of a linear scan useful for obtaining quantitative data about a sample which has shown interesting features in a two-dimensional scanning micrograph; this technique is also the obvious method for examining one-dimensional samples, for example, strands of hair. Samples need not be cut into thin sections but may be prepared arbitrarily thick, since the proton microprobe detects x-rays emitted only from the top 25 to 50 μm of the specimen. We illustrate here the application of this technique to (i) trace element distributions in single strands of hair and (ii) electrolyte distributions in frozen hydrated eye and kidney specimens.

The measurement of trace element concentrations in hair or nail tissue as a function of distance along the growth direction can provide a measure of the body's uptake of heavy metals or other relatively rare chemical constituents as a function of time; it may also reflect biochemical changes in the whole organism. The techniques of chemical analysis, atomic absorption spectroscopy, and neutron activation (*2*) have been used to determine the trace element content in short lengths of hair or nail tissue analyzed separately; these methods exhibit poor spatial resolution and insensitivity to certain elements. What is needed is a simple nondestructive method, sensitive to many elements simultaneously, with good spatial resolution. Major advances in this direction have been made with the use of electron microprobe analysis and x-ray fluorescence (XRF) analysis (*3*).

The scanning proton microprobe, with its intense collimated beam and low background signal, combines some of the advantages of both techniques, allowing one to analyze a single strand of hair with high spatial resolution (corresponding to a fraction of a day's growth), and high sensitivity simultaneously for most elements heavier than sodium (*4*). Because of the difficulty of aligning separate hairs and because of variations in the growth rate of individual hairs (*5, 6*), it is essential that only a single strand of hair be used if high spatial resolution is to be attained. We have analyzed hairs from an individual poisoned by ingesting methylmercury-treated seed grain in Iraq and from a victim of accidental arsine inhalation (*7*). The technique is straightforward: a hair is cemented to a rigid strip of Kapton with Kodak Micro Resist 747 (both materials are radiation-resistant, stable at high temperature, and relatively free of heavy element contamination), then scanned repeatedly past the proton microbeam by a lead screw assembly driven by a stepping motor. Proton-induced x-rays corresponding to each element of interest are detected and stored in a multichannel analyzer as a function of sample position. Thus one simultaneously obtains graphs of the abundance of a number of elements versus position along the hair. Typically, a current of 5 na of 2-Mev protons collimated to a beam diameter of 100 to 150 μm is used.

Figure 1a shows arsenic and zinc distributions obtained in this way from a strand of hair taken from the arsine-poisoned patient 183 days after inhalation. The arsenic peak is about 0.15 cm wide (corresponding to 5.1 days), located approximately 5.6 cm from the root. A simultaneous drop in the zinc content is followed by a slower recovery (25 days) to normal concentrations, an effect not previously reported to our knowledge. The iron concentration does not change, demonstrating that the zinc effect is not an artifact of the technique. Another hair taken from the patient 19 days after inhalation showed an almost identical pattern, both in the peak arsenic content and the corresponding drop in the zinc content. On the basis of several methods of calibration, we estimate the peak arsenic concentration to be ~ 200 μg/g.

Successive 1-cm hair segments taken at the same two times were also studied by